6324 J. Med. Chem. 2009, 52, 6324–6334
DOI: 10.1021/jm900358q

Journal of Medicinal Chemistry Article

Structure-Based Design of DevR Inhibitor Active against Nonreplicating *Mycobacterium tuberculosis*

Rajesh Kumar Gupta,[†] Tejender S. Thakur,[‡] Gautam R. Desiraju,*[,‡] and Jaya Sivaswami Tyagi*[,†]

[†]*Department of Biotechnology, All India Institute of Medical Sciences, New Delhi 110029, India, and* [‡]*School of Chemistry, University of Hyderabad, Hyderabad 500 046, India*

Received March 22, 2009

Antitubercular treatment is directed against actively replicating organisms. There is an urgent need to develop drugs targeting persistent subpopulations of *Mycobacterium tuberculosis*. The DevR response regulator is believed to play a key role in bacterial dormancy adaptation during hypoxia. We developed a homology-based model of DevR and used it for the rational design of inhibitors. A phenylcoumarin derivative (compound **10**) identified by in silico pharmacophore-based screening of 2.5 million compounds employing protocols with some novel features including a water-based pharmacophore query, was characterized further. Compound **10** inhibited DevR binding to target DNA, down-regulated dormancy genes transcription, and drastically reduced survival of hypoxic but not nutrient-starved dormant bacteria or actively growing organisms. Our findings suggest that compound **10** "locks" DevR in an inactive conformation that is unable to bind cognate DNA and induce the dormancy regulon. These results provide proof-of-concept for DevR as a novel target to develop molecules with sterilizing activity against tubercle bacilli.

Introduction

The consequence of tuberculosis infection is an outcome of the dynamic interplay between *Mycobacterium tuberculosis* (*M. tb*[a]) and the host immune defense. In most instances, an effective immune response by the infected individual results in bacterial containment within granulomas and the cessation of disease progression. Clinical studies suggest that the bacilli within granulomas are not killed but remain dormant in untreated individuals, causing latent infection that can last a lifetime.[1,2] Approximately 10% of latent infections reactivate, resulting in active disease months to years after the initial infection.[1,2] Conventional antitubercular therapeutic regimens target rate-limiting steps in metabolic pathways and enzymes that are unique to prokaryotes such as cell-wall biosynthesis (e.g., isoniazid) and RNA synthesis (e.g., rifampicin). These classes of drugs have maximal activity against actively dividing bacilli. Their lower efficacy against slow-growing and nonreplicating tubercle bacilli could explain why treatment regimens take so long to eradicate infection.[3] Therefore one of the priorities in tuberculosis research is to provide an intervention that targets clinically latent infection as an essential addition to current therapeutic regimens.[4]

The discovery of genes that play key roles in mycobacterial persistence has paved the way toward identifying novel targets unique to persistent organisms. Two-component regulatory systems belong to this class of novel targets.[5−7] These signaling systems play a major role in mycobacterial adaptation to the environment. DevR-DevS/Rv2027c[8] (also called as DosR-DosS/DosT) two-component signaling system (TCS) mediates the genetic response of *M. tb* to hypoxia,[9] nitric oxide,[10,11] and carbon monoxide.[12,13] These conditions are thought to be associated with bacterial dormancy development in vivo.[14,15] During bacterial adaptation to hypoxia and other stress signals, DevR response regulator mediates the induction of ∼48 genes that make up the DevR dormancy regulon.[9] To the best of our knowledge, mycobacterial TCSs have not been exploited for developing antimycobacterial agents. TCS are not found in mammalian cells, making this an important new target for developing novel antibacterial agents.[5,6,16] In view of the role of DevR in dormancy regulon expression and in hypoxic survival,[9,17] the identification of compounds that target the DevR-DevS/DosT TCS is likely to provide novel antitubercular chemotherapeutic agents against persistent organisms.[7,16,18] In the present study, a homology-based model of DevR was generated for use in rational inhibitor design. A set of structurally diverse potential inhibitor molecules chosen by in silico screening and docking was subjected to biological testing. Compound **10** was active in pathway-specific assays and prevented DevR binding to target DNA without inhibiting its phosphorylation, inhibited DevR-dependent transcription, and abrogated the survival of hypoxic but not aerobic or nutrient-starved *M. tb* cultures. The likely mode of compound **10** action is that it "locks" DevR in a conformation that cannot bind to cognate DNA and initiate subsequent DevR-mediated adaptive responses. Thus DevR regulator holds promise as a new and novel target for developing molecules effective against dormant tubercle bacilli.

*To whom correspondence should be addressed. For J.S.T.: phone, +91 11 26588491; fax, +91 11 26588663; E-mail, jstyagi@aims.ac.in. For G.R.D.: phone, +91 80 22933311; fax, 91 80 23602306; E-mail, gautam_desiraju@yahoo.com; present address, Solid State and Structural Chemistry Unit, Indian Institute of Science, Bangalore 560 012, India.

[a] Abbreviations: *M. tb*, *Mycobacterium tuberculosis*; TCS, Two-component signaling system; MOE, molecular operating environment; *E. coli*, *Escherichia coli*; MD, Molecular dynamics; EMSA, electro mobility shift assay; PZA, pyrazinamide.

 Published on Web 09/30/2009

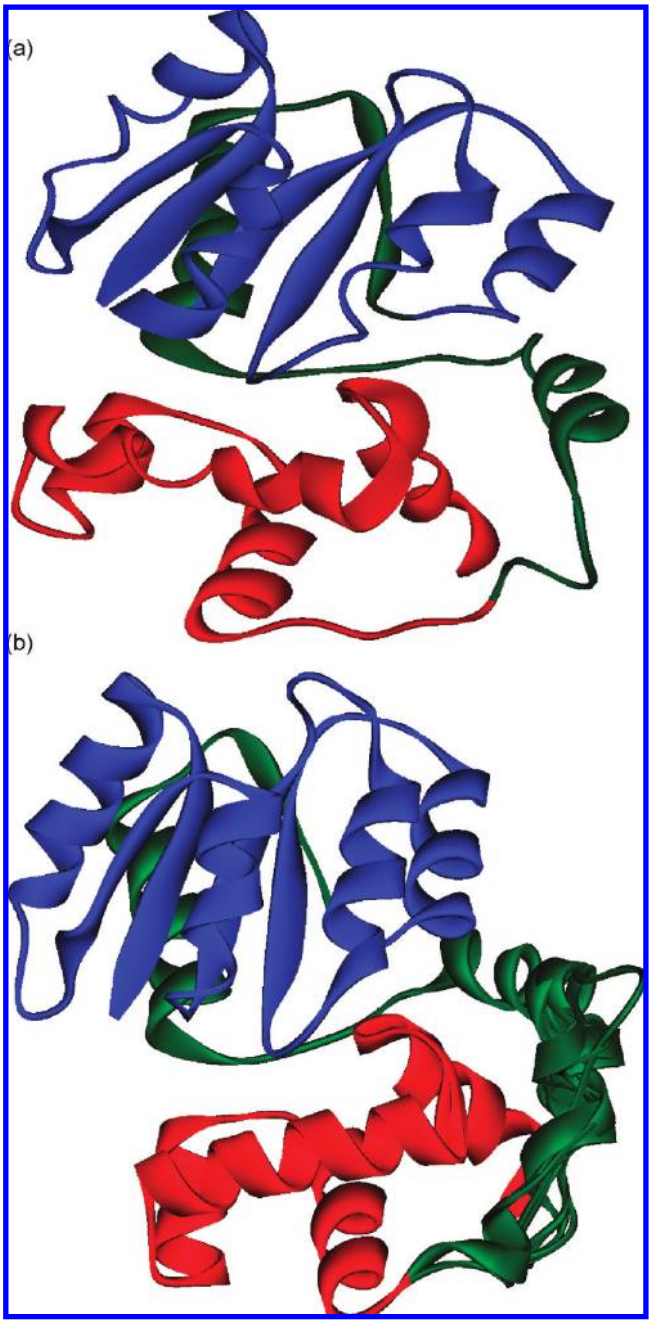

Figure 1. Homology model of DevR. (a) Composite model obtained from 1A04 (NarL of *E. coli*) and 1ZLK (*M. tuberculosis* DosR C-term crystal structure) templates. (b) Overlay of top 10 predicted homology models showing high variability in the linker region. N-terminal region shown in blue, linker region in green, and C-terminal region in red.

Results

Homology Modeling of DevR Protein. It is well-known that proteins of the response regulator family exist in active and inactive forms and that the structures of the two forms may be quite different. It is therefore ideal to model the structure of the active form of DevR with homology modeling because the binding of DNA occurs to the active form. The difficulties inherent in such an effort are obvious. The full amino acid sequence (1−217 residues) of DevR was used as a query to search the molecular operating environment (MOE software) homology data bank. This procedure revealed that the closest homology (32% sequence identity; Supporting Information pp S21−S22) was obtained with *Escherichia coli* (*E. coli*) response regulator NarL (PDB ID: 1A04). Accordingly, and realizing the inadequacies of a simple homology model when active and inactive forms of the protein are involved, a composite model was built using 1A04 as the primary template for the N-terminal region and the DosR structure (PDB ID: 1ZLK)[19] as the template for the C-terminal region of DevR (Figure 1a). Notably, the C-terminal domain of this DosR structure corresponds to the active form of the protein. The homology-based model was subjected to stepwise energy minimization in order to remove the overlapping regions (hydrogen atoms, side chains, backbone, and finally full protein). In addition, the structures were subjected to a small 200 ps molecular dynamics run in MOE using NVT ensemble. The model shows an rmsd of 0.81 Å for the 1ZLK protein region and 1.68 Å for the 1A04 protein region. An MOE-consensus check identifies the region between the 132 and 145 amino acids as a domain of high variability which occurs within the so-called linker region and which has been defined as spanning residues 98−149.[20] The high flexibility and variability of the linker region leads to a concomitantly low reliability in the prediction of structure of this domain (Figure 1b). Interestingly, the linker region of response regulator proteins is known to undergo large structural rearrangements during activation and the extent of conformational change varies from one response regulator family to another.[21] Thus it should be appreciated that the region of DevR, which is likely to be significant from the functional point of view, is the one which is obtained with the least reliability in the homology modeling exercise. Additionally, the overall poor sequence identity of 32% adds to the difficulty of the problem. For detailed modeling parameters see Supporting Information.

Identification of a Large Binding Pocket. The composite homology model (Figure 1a) was chosen for structure-based studies. The flowchart of the adopted virtual screening methodology is given in Figure 2. It was searched for available binding pockets that were ranked by size and hydrophobicity scores (see Supporting Information for details). The largest pocket defined by 23 residues (Figure 3a) was chosen as a target for inhibitor design. This pocket includes residues from the β4−α4 region of the N-terminal domain, the α6 helix of the linker domain, and the α8 and α10 helices of the C-terminal domain. The chosen active site was subjected to molecular surface analysis to analyze the nature of the binding pocket. A Gaussian contact surface that surrounds the van der Waals surface of the protein active site atoms was created to visualize hydrophobic and hydrophilic regions in the pocket (Figure 3a). Gaussian surface analysis of the pocket revealed the highly hydrophobic nature (green) of the active site. Hydrophilic patches (purple) were seen around Arg77, Ala98, Ser99, Ser123, Arg192, and Thr205 residues, suggesting that these amino acids could play an important role in ligand binding through hydrogen bonding and other polar interactions.

Pharmacophore-Based Virtual Screening. Nonavailability of definitive structural information related to the active site and of potent ligands at the time this study was conducted made it difficult to initiate a rational approach to explore probable inhibitors for DevR protein. In addition to this, poor reliability of the homology model and large conformational flexibility aggravated the prevalent situation. To address these issues, a novel strategy was designed to ascertain

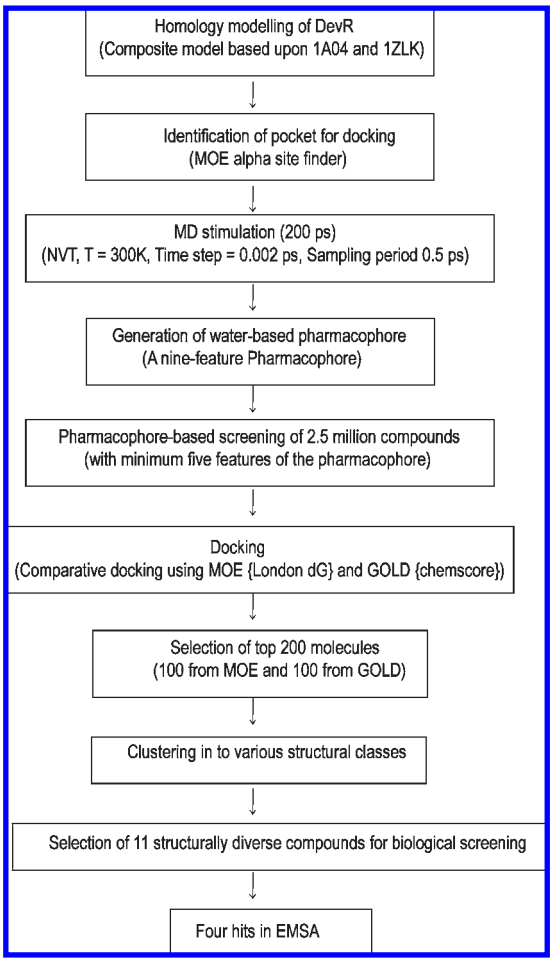

Figure 2. Methodology for homology modeling of DevR, pharmacophore-based virtual screening, docking, and selection of compounds for biological testing.

the ligand−protein binding mode by using water−protein interactions that were retained during the dynamics run. A simple water-based pharmacophore query was built by examining the robust water−protein contacts during the molecular dynamics (MD) run by random sampling of MD structures (see Supporting Information for details). An overlay of the active site of the 10 sampled structures is shown in Figure 3b. Upon the basis of the water to protein contacts, a model was generated with a nine-feature pharmacophore consisting of two hydrogen bond acceptors (F1, F2), three hydrogen bond donors (F3, F4, F5), and two donor/acceptor points (F6, F7). Two additional hydrophobic features were manually added based upon the active site analysis; feature F8 was added in the region surrounded by residues Val118, Leu124, and Thr198 and feature F9 was chosen between residues Leu125, Leu135, Leu137, and Ile194 (Figure 3b,c). This pharmacophore query was used to screen a preprocessed (using fingerprinting and drug like descriptors) library of compounds obtained from the Zinc Database (Zinc5−2.5 million)[22] to get a reasonable sized data set of structurally diverse molecules with a minimum of five pharmacophore features (see Figure S3 in Supporting Information).

Docking and Ranking of Screened Data Set Molecules. The MOE-Dock Box was created around the selected pocket using dummy atoms generated based upon alpha spheres, and the least energy conformations of each molecule were docked in the pocket. A comparative docking of the selected ligands obtained from the initial pharmacophore screening was also performed with GOLD. The top 100 docked hits obtained from each of MOE-Dock (London dG) and GOLD (Chemscore fitness function) are shown (Supporting Information Table S1).

Selection of Compounds for Biological Testing. Eleven structurally diverse compounds were selected for biological screening. A compound was selected if at least one of the following criteria was met: its presence in the top 100 hits obtained from both GOLD chemscore and MOE dG scoring functions (compounds **2**, **4**, **5**, and **7**), a high score either in MOE or in the GOLD dock score ranking (compounds **1**, **3**, **6**, **8**, **9**, **10**, and **11**), structurally diverse nature (to the extent possible) compared to the other compounds selected, availability of the molecule with the vendor (Table 1). The structures of these 11 compounds and of their analogues are given in Supporting Information Table S2. Compound **10** (MOE Rank 1) was characterized in greater detail using biological assays. Its structure and docking in the selected pocket is shown in parts d and e of Figure 3.

Inhibition of DNA Binding Property of DevR. Because phosphorylated DevR binds to DNA, we first tested whether compound **10** affected DevR phosphorylation. It did not interfere with the generation of active DevR species by phosphorylation, which enabled us to assess the effect of selected compounds **1**−**11** on DevR binding ability by EMSA (Figure 4a). Compounds **1**, **2**, **3**, **4**, **6**, **9**, and **11** did not inhibit the binding of phosphorylated DevR protein to *fdxA* promoter DNA. By contrast, **5**, **8**, and **10** completely abrogated DNA−protein interaction at 250 μM while compound **7** inhibited 100% binding only at 500 μM. Compounds **5**, **7**, and **8** inhibited DevR binding to DNA with IC_{50} of 145, 99.0, and 84.2 μg/mL, respectively (Table 1), and compound **10** inhibited DevR binding to DNA with an IC_{50} < 26.2 μg/mL (Figure 4b). Because phosphorylation is known to trigger conformational changes in response regulators of the NarL family during activation,[23] the order of compound **10** addition was next assessed to understand whether the binding pocket was altered by phosphorylation. Compound **10** inhibited DevR binding to DNA in EMSAs when added before or after DevR phosphorylation (not shown). Compound-mediated inhibition of DevR binding to DNA was established to be specific because compound 10 failed to prevent the binding of HupB, a DNA binding *M. tb* protein, to DNA (Figure 4c).

Inhibition of DevR Regulon Gene Expression by Compounds. DevR positively autoregulates its synthesis at the transcriptional level by interacting with Dev boxes in the *Rv3134c* promoter of the *Rv3134c-devRS* operon.[24] Therefore, inhibition of *Rv3134c* promoter activity was used as a measure of anti-DevR activity of those compounds that interfered with DevR−DNA interaction. Promoter activity was inhibited by 50% in the presence of 250 μM of compounds **5** and **10** and by ∼30−40% in the presence of compounds **7** and **8** (Figure 4d). Compound **10** inhibited the activity of other DevR-regulated promoters as well, namely *narK2* and *hspX*; all three promoters were inhibited with an IC_{50} < 65.5 μg/mL (Figure 4e). The action of compound **10** was specific, as it did not inhibit constitutive *sigA* promoter activity. However, compounds **5**, **7**, and **8** also inhibited *sigA* promoter activity (Figure 4d).

Sterilizing Action of Compound 10 on Hypoxic but Not Nutrient-Starved Dormant or Aerobic Cultures. Hypoxia-induced nonreplicating persistence is a commonly used model

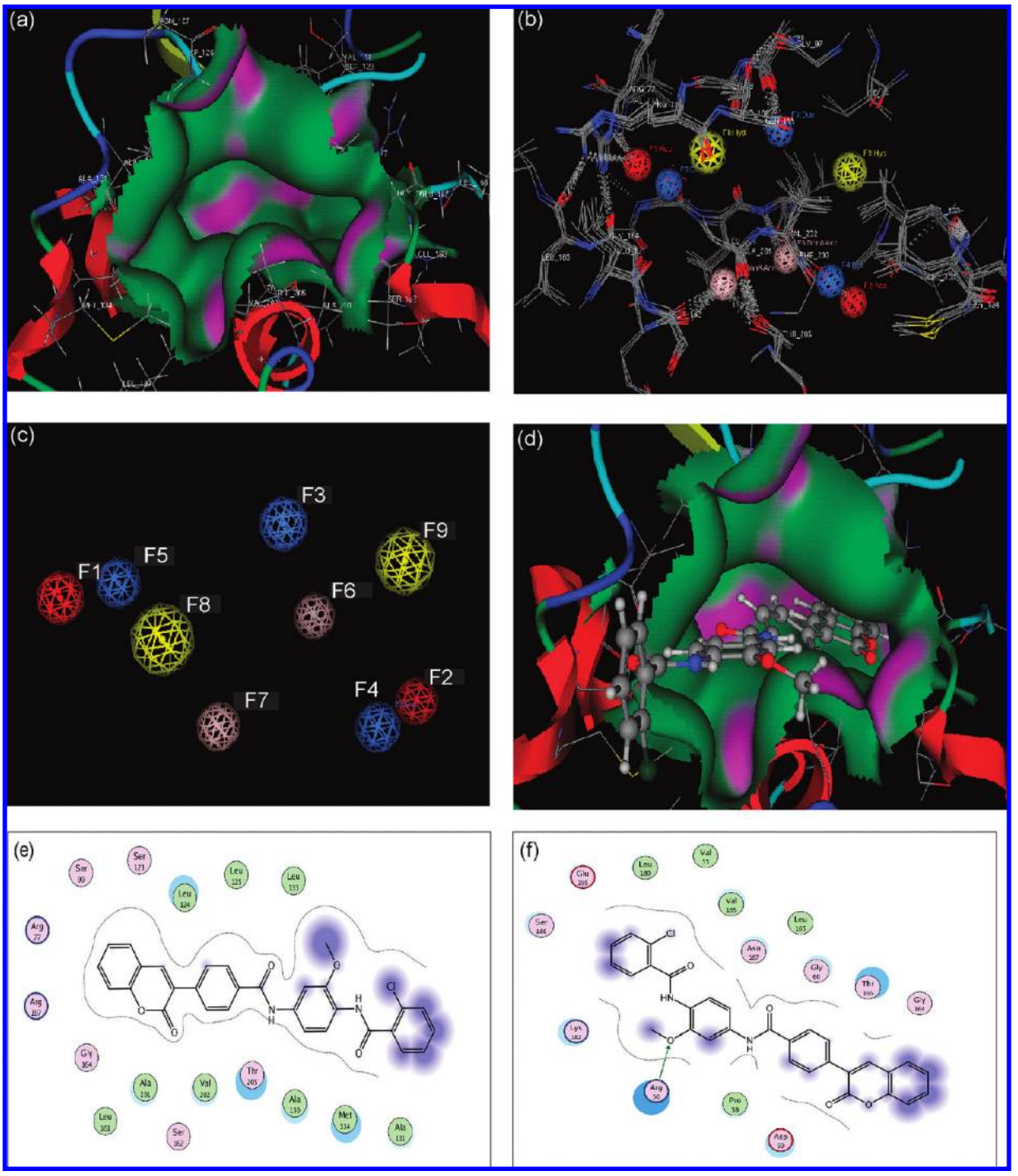

Figure 3. (a) Pocket (defined in Supporting Information Table S6) selected for docking of compounds. Various surface properties are indicated, namely H-bonding (purple), hydrophobicity (green). (b) Overlay of 10 sampled structures obtained from the molecular dynamics run showing pharmacophoric points chosen based on water−protein contacts. Hydrogen bond trace is shown in gray. Red sphere represents an acceptor feature, blue sphere represents a donor feature, pink sphere represents donor/acceptor feature. Hydrophobic feature is shown in yellow. (c) Nine feature water-based pharmacophore used for initial database screening. (d) Compound **10** docked in pocket. (e) Two-dimensional structure of compound **10** in pocket of DevR homology model. (f) Two-dimensional structure of compound **10** in pocket of DevR crystal structure.

of *M. tb* dormancy in vitro,[14] and DevR plays a key role in bacterial adaptation in this model.[17] When compound **10** was added at 131 μg/mL concentration on day 0 to cultures (Format H1), bacterial viability was reduced by >99% (4 log reduction, Figure 5a). By contrast, bacterial viability was not inhibited when compound **10** was added on day 30 to hypoxia-adapted cultures in format H2 (Figure 5b). As expected, hypoxia-adapted cultures were susceptible to metronidazole (M) and metronidazole plus isoniazid (M + I) but not to isoniazid (Figure 5b).

The sterilizing activity of compound **10** was assessed by use of enriched broth to revive hypoxia-adapted cultures under aerobic conditions. Compound **10**-treated format H1 cultures (131 μg/mL) failed to revive even after 30 days, while cultures exposed to lower concentrations recovered partially after an initial lag period (shown up to 20 days, Figure 6a).

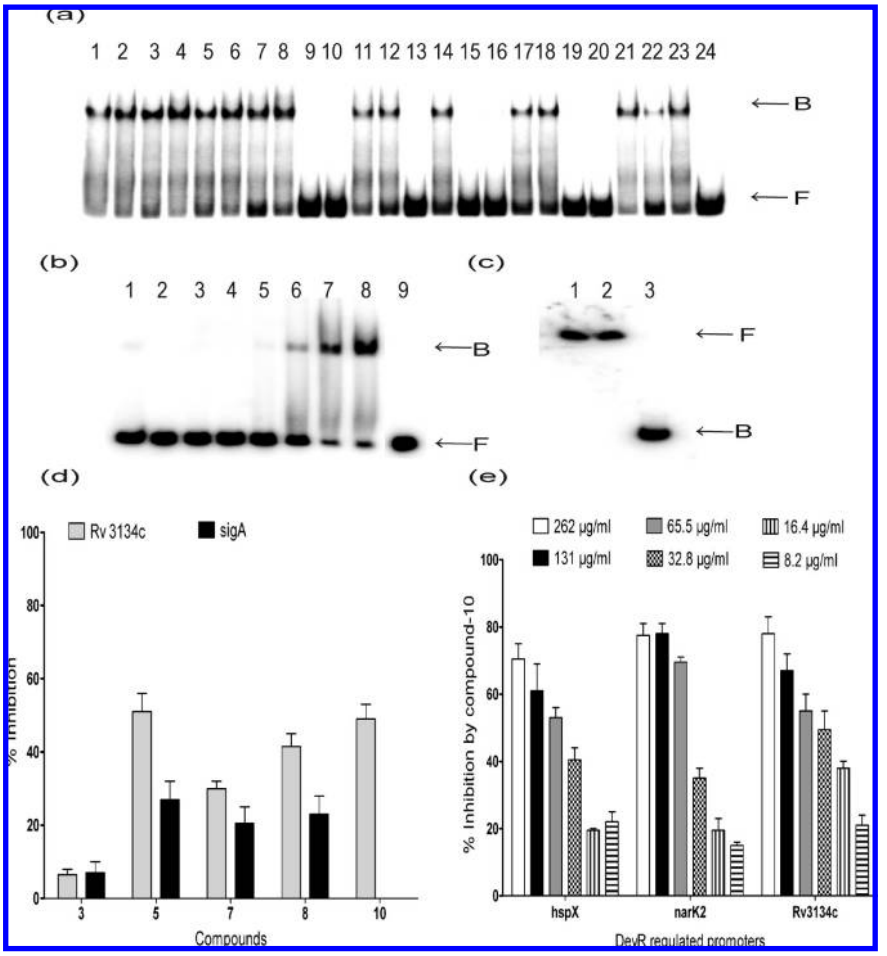

Figure 4. Effect of test compounds on DevR binding to *fdxA* promoter DNA in electro mobility gel shift assay. (a) Compounds **1**−**11** were tested at 500 and 250 μM concentrations, respectively. Lanes 1, 2, compound **1**; lanes 3, 4, compound **2**; lanes 5, 6, compound **3**; lanes 7, 8, compound **4**; lanes 9, 10, compound **5**; lanes 11, 12, compound **6**; lanes 13, 14, compound **7**; lanes 15, 16, compound **8**; lanes 17, 18, compound **9**; lanes 19, 20, compound **10**; lanes 21, 22, compound **11**; lanes 23, 24, positive control and free DNA. (b) Lanes 1−7 represent 262, 209.6, 157.2, 104.8, 52.4, 26.2, and 13.1 μg/mL of compound **10**, respectively; lanes 8, 9, positive control and free DNA respectively. (c) Effect of compound **10** on HupB binding with *fdxA* promoter; lane 1, 500 μM of compound **10**; lanes 2, 3 correspond to positive and negative controls. (d) Effect of compounds **3** (negative control), **5**, **7**, **8**, and **10** (250 μM each) on *Rv3134c* promoter activity in *gfp* reporter assay. (e) Effect of different concentrations of compound **10** on DevR-regulated promoters.

By contrast, compound **10**-treated cultures in format H2 (compound added on day 30) were not sterilized and recovered partially after an initial lag period. As expected, control and isoniazid-treated cultures revived under aerobic conditions although a slight lag in recovery of metronidazole-treated cultures was noted (Figure 6b). These results establish that addition of compound **10** (131 μg/mL) on day 0 interferes with bacterial adaptation necessary for hypoxic viability and leads to bacterial sterilization. The sterilizing action of compound **10** was specific for hypoxic cultures as it did not inhibit the growth or viability of aerobic *M. tb* culture (not shown).

To further confirm target specificity, the effect of compound **10** on *M. tb* gene expression and viability was tested in the nutrient starvation model wherein dormancy development is not mediated by DevR.[25] *Rv3134c* and *hspX* promoter activities were not induced in the starvation model (Supporting Information Figure S1) and was consistent with previous reports.[25] Compound **10** had no effect on mycobacterial viability in this dormancy model and thereby confirmed compound **10**'s specificity for DevR-mediated dormancy development pathway (Supporting Information Figure S1).

Predicted Interactions between Modeled DevR Structure and Active Compounds. To obtain biologically active conformations (poses), compounds **5**, **7**, **8**, and **10** (showing biological activity) were further docked into the selected pocket of homology model using the MOE-dock module. A total of 1000 conformations were generated for each of the molecules and docked and ranked based upon London dG binding free energy score. Ligand−protein interaction analysis of the top scored poses docked in the protein is given in Supporting Information Table S3. Hydrogen bond analysis shows involvement of only a few strong hydrogen bonds in the ligand binding. On the contrary, a large number of weak C···H···O and C−H···N hydrogen bonds were observed in all the docked poses of active molecules. Moreover, these poses showed a predominance of hydrophobic interactions between the aromatic rings (in compound) and the hydrophobic residues of the binding pocket. To identify the key residues responsible for ligand binding, a pixel hit map of the hydrogen bonds formed between ligand molecules and protein was generated. Active site residues Arg77, Ser99, Leu124, Leu125, Ala130, Gly164, Arg197, Thr198, and Ala201 were found to be mostly involved in interaction with bioactive ligands (Supporting Information Figure S2).

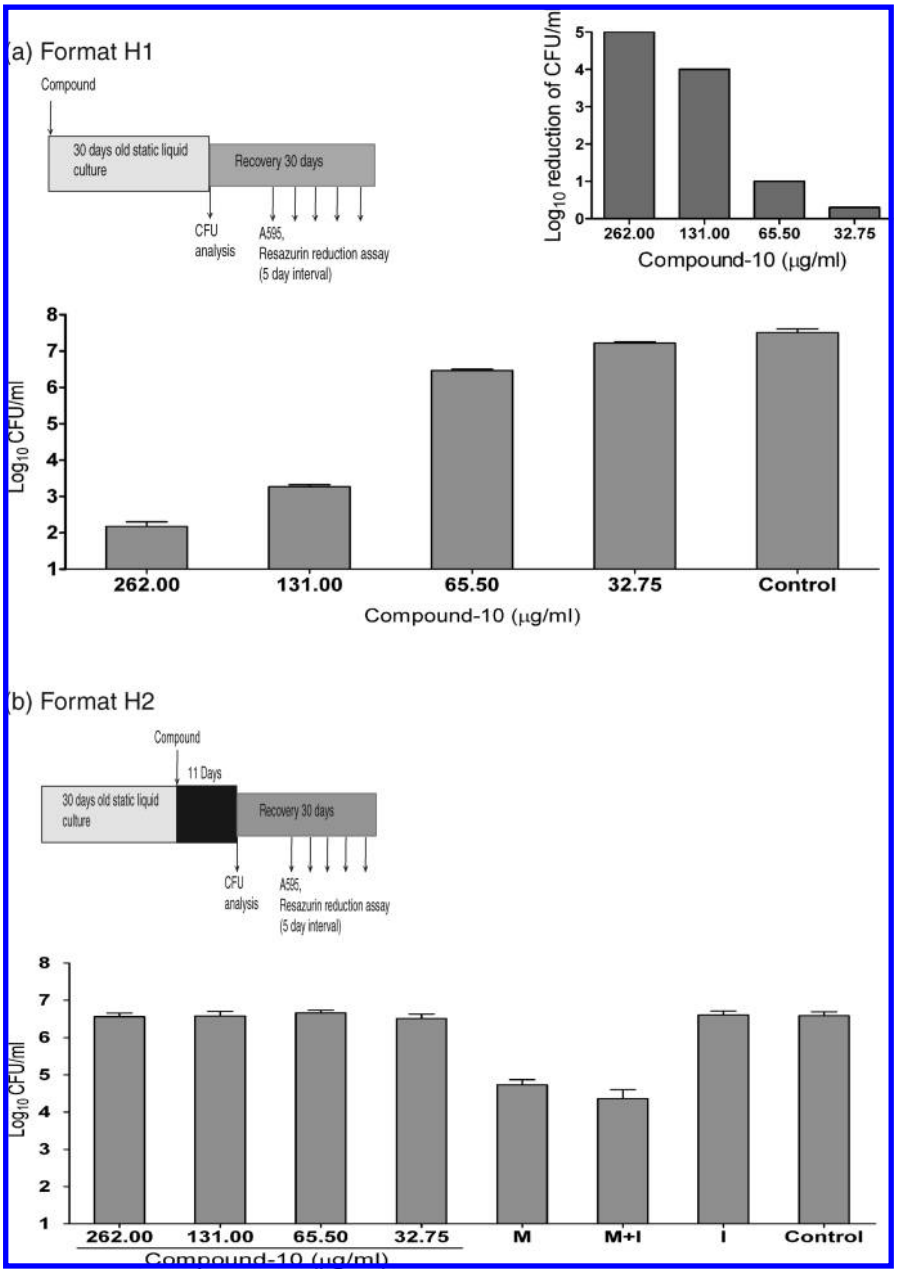

Figure 5. Effect of compound **10** on viability of hypoxic *M. tuberculosis* cultures. (a) Format H1. (b) Format H2. M, metronidazole; I, isoniazid; control, contains equal concentration of DMSO.

Prediction of Minimal Essential Pharmacophore Features of Inhibitor. As we were quite successful in obtaining a candidate inhibitor using modeled DevR protein, the structures of the potent molecules were reanalyzed. Assuming that the active molecules bind to the same pocket in a similar fashion, a qualitative pharmacophore of important structural features was generated using the MOE pharmacophore elucidation module. Of the four active molecules, compound **8** was not considered for pharmacophore elucidation owing to its structural similarity with active compound **10**. Various conformations for each of the active compounds (**5**, **7**, **10**) were generated using a rule-based systematic search of specific torsion angles for all of the rotatable bonds present in the molecule and aligned to obtain the most common pharmacophore feature using the MOE-pharmacophore elucidation module. The pharmacophore with the highest alignment score is shown in Supporting Information Figure S3. The ligand-based pharmacophore shows that five points are essential to describe the activity of molecule: two hydrogen bond acceptors (F1 and F2), one donor (F3), and two hydrophobic/aromatic features (F4 and F5). The presence of one acceptor (F1) and one donor (F3) close to each other suggests strongly that the potent compounds have an amide functional group. A similar feature was found in the crude water-based pharmacophore used in initial screening of the database (Figure 3c).

Discussion and Conclusions

DevR is a key regulator of the hypoxia-induced dormancy response in *M. tb*. DevR-regulated genes are also strongly induced in vivo,[26−28] suggesting that it could be a good target for developing drugs against persistent organisms.[16,18,19] Structure-based virtual screening is often used to identify candidate inhibitors from among large compound libraries.

Table 1. Bioactivity, Ranks (MOE and GOLD), and Structures of the Selected Compounds[a]

Compound Code	Molecular Wt.	MOE Rank	Gold Rank	Bioactivity		Structure
				IC_{50} EMSA*	IC_{50} GFP¶	
1	362	24	-	Nil	Nil	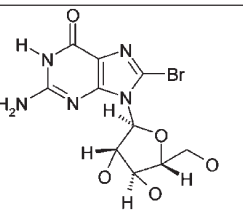
2	276	73	67	Nil	Nil	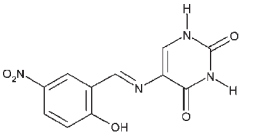
3	283	-	65	Nil	Nil	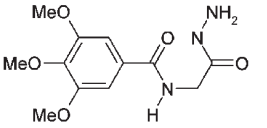
4	449	38	37	Nil	Nil	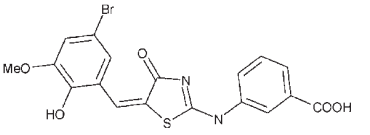
5	488	59	09	144.9	122.0	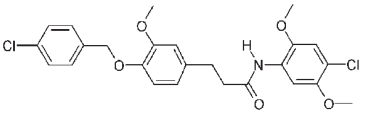
6	424	-	18	Nil	Nil	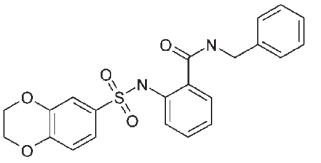
7	396	66	47	99.0	118.8	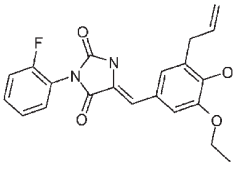
8	420	-	07	84.2	126.3	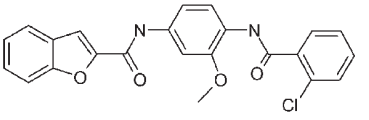
9	388	-	35	Nil	Nil	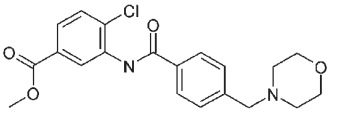
10	524	01	-	< 26.2	65.5	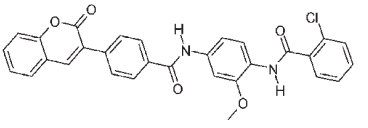
11	363	10	-	Nil	Nil	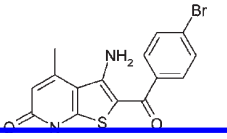

[a] * Inhibited binding of DevR to DNA by 50% (μg/mL). ¶ Inhibited DevR-dependent promoter activity (GFP fluorescence) by 50% (μg/mL).

When this study was initiated, the crystal structure of only the C-terminal domain of DevR was available.[19] Therefore, a composite homology model was built and subjected to virtual screening for potential DevR inhibitors. The main feature of

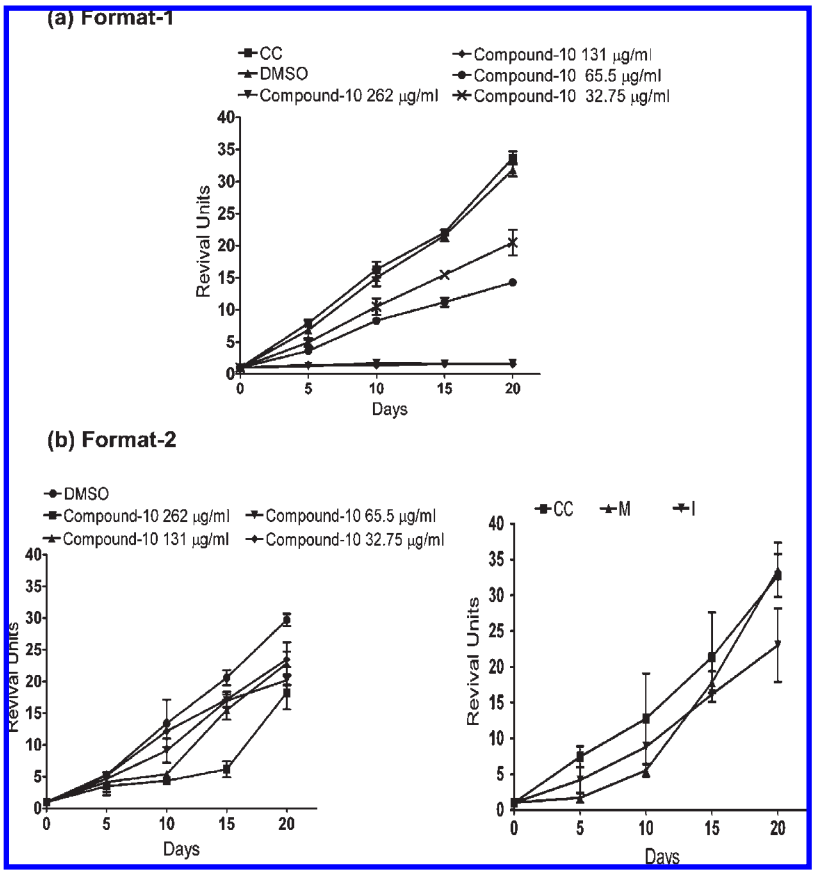

Figure 6. Revival of compound **10**-treated *M. tuberculosis* hypoxic cultures. (a) Format H1. (b) Format H2. M, metronidazole; I, isoniazid; CC, culture control; DMSO, contains equal concentration of DMSO as test compound. Revival is represented on a scale of 1 to 40, where an arbitrary value of 1 was assigned to zero day cultures.

this work is the identification of a substituted phenylcoumarin, compound **10**, that specifically inhibits DevR activity and function and drastically reduces the hypoxic survival of *M. tb* by 4 logs. Pathway specificity of compound **10** is supported by several observations: it inhibited binding of DevR, but not HupB, to DNA; it inhibited DevR-regulated but not *sigA* promoter activity; it interfered with the viability of hypoxic but not that of either aerobic *M. tb* cultures or dormancy-adapted cultures in the nutrient starvation model. This is consistent with the available knowledge that DevR is not essential for aerobic growth or adaptation to nutrient starvation.[25]

Sterilizing Activity of Compound 10. The sterilizing action of compound **10** on *M. tb* was established by the recovery assay. Its action is in contrast to that of conventional antitubercular drugs whose antibacterial activity diminishes in hypoxia-induced dormancy. Our findings collectively suggest that interfering with DevR during the early stages of bacterial adaptation to oxygen limitation is a novel and effective means to target dormant or nonreplicating organisms. Compound **10**-mediated bacterial sterilization was noted in format H1 but not in format H2. A possible explanation could be that in the former, compound **10** efficiently bound to DevR target protein and prevented its positive autoregulation and subsequent activation of the dormancy regulon. In format H2, hypoxia-adapted bacteria accumulate DevR to higher levels due to induction[9,24] and the addition of compound **10** to adapted cultures failed to completely neutralize DevR function due to stoichiometric insufficiency. An alternate explanation for the failure to observe compound **10** activity in format H2 is that DevR may be required during the early stages of adaptation to hypoxia as suggested recently.[29]

Isoniazid, rifampicin, ethambutol, and pyrazinamide (PZA) are the mainstay of antitubercular regimens worldwide. In spite of a high MIC, PZA is a cornerstone of TB chemotherapy as it shortens the duration of therapy from 9 to 12 months to 6 months by killing a population of semidormant tubercle bacilli that are not cleared otherwise.[30] PZA is proposed to target membrane energetics as a mechanism of action.[31] The challenges of high MIC and drug resistance to PZA underscore the need to develop alternative molecules with unique mechanism of action against semidormant and dormant bacteria. Diarylquinolines are promising new molecules that target ATP synthase and have bactericidal activity against both aerobic and dormant mycobacteria.[32,33] Here we show for the first time that bacterial sterilization is achievable by disrupting DevR function. It is hoped that optimization and pharmacological investigation of compound **10** would lead to the development of potent drug candidates against dormant bacteria. An approach of combining molecules such as compound **10** derivative, diarylquinolines, and PZA, which target different bacterial components and act through different mechanisms of action, is likely to produce bactericidal synergism against recalcitrant nonreplicating subpopulation of *M. tuberculosis*.

Utility of Water-Based Pharmacophore. The key challenge in molecular modeling of DevR is that the protein exists in active and inactive forms with widely different conformational features, and it becomes an issue to select those structural features that are biologically relevant. The linker

region between the N- and C-terminal domains is functionally very important, but there was not much structural information about it. In the absence of definitive structural information about the binding site, our novel strategy to use water-to-protein interactions (to identify pharmacophore points) as a crude filter was the crucial step in virtual screening and paid fruitful dividends. It helped to maximize our chances of obtaining an active molecule from the ligand database. Use of water−protein interactions worked successfully as a probe to spatially identify favorable hydrophilic regions for ligand binding inside the pocket with both hydrogen bond donor and acceptor features. Moreover, issues relating to system flexibility and temporal stability of ligand−protein interactions were best modeled using this approach. Retention of similar pharmacophore features in the ligands that were retrieved underscored the high efficacy of this simple approach used for screening. In this study a relatively short molecular dynamics run of 200 ps was carried out to derive binding site conformation and water distribution. However, proper care was taken for protein stabilization before setting up the molecular dynamics simulation and sampling of structures was done only after the protein was stabilized (this happened even after 100 ps). Further confidence in the pharmacophore's authenticity came from the identification of one biologically active molecule (compound **10**) from among the 11 screened compounds that were shortlisted from the docking exercise.

Comparison of Homology Model and X-ray Crystal Structure of DevR. The 3D structure of the nonphosphorylated (inactive form) of full-length DevR protein was published recently.[20] Although we had finished most of our studies by then, we found it meaningful to compare various structural and functional aspects of the modeled and experimental DevR structures in order to critically assess our computational approaches in designing inhibitors against this target. Comparison of the secondary structural elements in the N-terminal region shows a close similarity between the two structures except for the presence of a $\beta 5$ sheet in the homology structure. In hindsight, this difference appears to be obvious; the NarL template structure has a $(\beta\alpha)_5$ structural motif, which is a very common motif in the response regulator family,[34] but this is actually not present in the experimental structure.[20] In the absence of a suitable template with high sequence identity, the region defined by residues 99−103 was not predicted correctly (Supporting Information Table S4). Domain-wise rmsd analysis of the homology model with the X-ray crystal structure shows considerable deviation in the linker region when compared to the C- and N-terminal domains (Supporting Information Table S5). The homology model shows rotation of the α7−α10 helix bundle in the C-terminal domain around the α5−α6 linker helices with respect to the experimental crystal structure. The linker helices in the homology model are also folded inward when compared with those in the experimental structure.

With respect to the C-terminal region, it may be noted that although we had taken information for this domain from its X-ray structure,[19] the composite homology model still showed large deviations in the Cα atoms of the α10 helix compared to that of the experimental structure (which is inactive, Supporting Information Tables S4 and S5). Similar differences between inactive (experimental; 3C3W) and active (1ZLK) forms were pointed out recently by Hol's group.[20] This dilemma points out that there may be some fundamental structural differences between active and inactive forms of a protein and that every molecular modeling exercise involves, in its own way, a "leap of faith", hoping that a sufficiently critical amount of relevant information is being used in construction of the model. In the present case, our use of a water-based pharmacophore model appears to have been the critical ingredient in arriving at some compounds with high inhibitory activity.

DevR is believed to undergo an extensive helix rearrangement during activation.[20] Our experimental data provides valuable insights into the probable architecture of the native pocket; surprisingly, compound **10** does not inhibit DevR phosphorylation (activation) and yet it somehow prevents formation of the DNA binding active species. This implies that the pocket architecture is preserved in both inactive and active states of DevR protein (Supporting Information Figure S4). In the crystal structure, the pocket comprises residues from both N- and C- terminal domains (part f of Figure 3, Supporting Information Table S6); it includes residues from the α9 DNA binding helix, those involved in interdomain interactions and α10 helix region in the inactive protein (Supporting Information Figure S2), suggesting the possibility that bound compound **10** might prevent formation of the active conformer. In the absence of an active form structure for DevR, the best possible binding pocket was chosen computationally. Compound **10**, which secured the top rank in the MOE docking scheme, was also the most potent molecule identified in this study, further suggesting the computationally defined pocket to be a relevant binding site. Future challenges are to confirm the binding site and to analyze the proposed mechanism of inhibitor action by experimental approaches. We rationalize the computational and experimental data by considering the inhibition mechanism from the point of view of conformational selection rather than from an induced fit model.[35] Insights from the recent X-ray structural analysis of full-length inactive DevR protein[20] also favor the involvement of various protein conformations in the response regulation process. However, such a comparison remains elusive in the absence of a full crystal structure of the active form of DevR. In conclusion, highlighting our success in obtaining a specific inhibitor against DevR protein and by consideration of the activation mechanism proposed for DevR,[20] our findings suggest that inhibitor compound **10** "locks" DevR in a conformational state that does not transduce into the activated protein conformer essential for DevR activity during bacterial adaptation to hypoxia.

Experimental Section

Homology Modeling of 3D Structure of DevR, Pharmacophore-Based Virtual Screening, and Docking of Compounds. The tertiary structure of DevR was predicted by the homology modeling approach[36] using the molecular modeling package molecular operating environment (MOE 2006.08; Chemical Computing Group Inc., Montreal, Canada; www.chemcomp.com). Briefly, sequence alignments were obtained by using Clustal.[37] The superposition of the coordinates of Cα-atoms of the theoretical model with NarL as the template protein (1A04) was performed with the MOE-homology module. Problematic and overlapping regions of the built homology structures were analyzed with the help of MOE stereochemical check and by visual inspection of outliers from the Ramachandran plot and then rectified. The structural parameters were evaluated, and the prediction quality of the modeled structure was assessed. The homology model of DevR was searched for active sites with the MOE Alpha Site Finder.[38] A short 200 ps MD run

of water-soaked protein (with water layer width of 5 Å) was performed, and the nature of various hydrogen bond interactions between water molecules and the protein within the active site of DevR were studied using the in-house hydrogen bonding analysis tool (HBAT) software.[39] A total of 2.5 million molecules obtained from the Zinc database[22] (Zinc5, Jan 2005 release) were screened against the chosen active site in the modeled DevR structure using water-based pharmacophore query. Preprocessing of the ligand database was done using pharmacophore preprocessor using PCHD scheme annotation for the ligands. Screened ligands were docked within the chosen active site of the homology modeled protein with both MOE-Dock module and with GOLD (GOLD 3.0; Cambridge Crystallographic Data Centre: Cambridge, UK) docking software; the results obtained with these two software were compared. Selected hits obtained after virtual screening were subjected to biological testing. Detailed information on homology modeling of DevR, virtual screening, and docking of compounds is provided in Supporting Information.

Bacterial Strains and Growth Conditions. *M. tb* H37Rv was revived from −80 °C bacterial stocks and grown either in Dubos medium containing 0.1% Tween-80 and 10% (v/v) albumin dextrose complex (ADC) (referred to as DTA medium) or in Middlebrook 7H9 medium containing 0.1% Tween-80 and 10% ADC (MTA). All cultures were grown at 37 °C in a shaker incubator (190−220 rpm) unless mentioned otherwise.

Chemical Compounds. All the selected hits (compounds **1**−**11**) were purchased from Chembridge Corporation Limited, USA, and were reported to have a purity ≥90% by ^{1}H NMR. Compound **10** was analyzed by HPLC using reverse phase C-18 column and was determined to have a purity of >95%.

Electromobility Shift Assay (EMSA). N-terminal GST-tagged DevR was purified as described.[40] *fdxA* promoter DNA probe was generated by PCR from *M. tb* DNA using ^{32}P end-labeled oligonucleotide primer FdxAF (TGACGGGCTATCGTAAGTTTATG) and FdxAR (CACGCACTCACTACCGATCACA). Activated DevR was generated by phosphorylation with acetyl phosphate and used in EMSA as described.[24] Briefly, DevR∼P (1 μM final concentration) was preincubated for 10 min at 30 °C in the phosphorylation reaction in the presence and absence of test compounds. Labeled DNA (∼2 ng) was added to the reaction and further incubated on ice in binding buffer for 30 min. DNA−protein complexes were analyzed by electrophoresis as described.[24] Purified HupB protein (generous gift from Prof. H. K. Prasad, New Delhi) was used in EMSA as described above.

GFP Reporter Assay. *M. tb* harboring various DevR-regulated *gfp* reporter promoter plasmids were used to assess the activity of various compounds as described.[24] Initial compound dilutions were prepared in dimethyl sulfoxide and subsequent 2-fold serial dilutions were in 0.1 mL of DTA medium in microplates. *M. tb* stocks were cultured in DTA medium up to midlogarithmic phase (OD_{595} ∼ 0.4) under shaking conditions, diluted in the same medium (OD ∼ 0.05), and dispensed in 100 μL aliquots per well. Control wells contained only compound, bacteria, or medium. The plates were incubated for 48 h, and GFP fluorescence was measured as described.[24] GFP fluorescence due to promoter activity was calculated by subtracting background fluorescence of vector and compounds. Results are expressed as mean ± SD percent inhibition $[1 - (RFU)_{compound}/RFU_{DMSO}) \times 100]$ from three independent experiments each in triplicate wells.

***M. tb* Aerobic Viability Assay (REMA Assay).** Antimicrobial activity of compounds on aerobic *M. tb* culture was tested in triplicate cultures as described.[41] Plates were incubated for 7 days. Thereafter, Resazurin (30 μL of 0.02%) and Tween-80 (12.5 μL of 20%) were added to each well. Wells were observed after 48 h for a color change from blue to pink. Fluorescence was measured in a spectrofluorimeter with excitation at 530 nm and emission at 590 nm.

***M. tb* Viability Assay in Hypoxia Model of Dormancy (HyRRA Assay).** Briefly, *M. tb* stocks were grown in Dubos medium until logarithmic phase (OD_{595} ∼ 0.4) and further diluted to an OD_{595} of 0.003. Culture aliquots of 2 mL were injected into 4 mL vacutainer tubes with self-sealing caps and kept static for hypoxia to set in as described.[41] Format H1: compounds were injected into tubes on day 0, and the cultures were incubated until methylene blue decolorized (indicating anaerobiosis, typically ∼30 days). Format H2: compounds were added to 30 days-old nonreplicating dormant cultures and incubated further for 11 days. Metronidazole (M) and isoniazid (I) were used as controls to assess drug susceptibility of anoxic and aerobic cultures, respectively. After 30 days and 41 days (for formats H1 and H2, respectively), conventional CFU analysis was performed on culture aliquots by serial dilution plating. Resazurin (300 μL of 0.02%) and Tween-80 (70 μL of 20%) were injected into the remaining culture in each tube, vortexed, and incubated overnight prior to determination of MICs and bacterial viability by HyRRA.[41]

Revival Assay for Hypoxia-Adapted Cultures. At 30 days and 41 days under formats 1 and 2, respectively, cultures were pelleted at 11000*g*, washed with Middlebrook 7H9 medium, resuspended in 4 mL of the same medium supplemented with 5% OADC and 0.1% Tween-80, and grown under aerobic shaking conditions (190 rpm in 50 mL tubes). Aliquots of 200 μL were withdrawn from each tube at 5 day intervals to monitor the recovery of dormant cells by resazurin reduction assay and OD_{595} measurement. Similar results were obtained by both assays.

Nutrient Starvation Model of Dormancy. GFP reporter assay: *M. tb* strains harboring *Rv3134c*/*sigA* promoter *gfp* reporter constructs were grown to OD_{595} ∼0.40 in MTA medium under shaking conditions. Cells were pelleted at 5000 rpm, washed twice with phosphate buffer saline (PBS), and resuspended in either PBS or MTA medium. Cultures were diluted to OD_{595} ∼ 0.02 and 1 mL aliquots were incubated in 2 mL cryovials. Cultures aliquots of 200 μL were withdrawn at one week intervals into black clear-bottomed 96-well microplates and GFP was measured as described above. Viability assay: Compounds were tested in a nutrient starvation model as reported[25] using the culture setup described above. Viability was assessed in two formats: in format N1, compounds were added on day 0 and incubated for 6 weeks. In format N2, compounds were added to six-weeks-starved cultures and incubated for 11 days (Supporting Information Figure S1). Control cultures containing 1.5 μg/mL of methylene blue did not decolorize and confirmed that oxygen was not depleted in the nutrition starvation model. For viability determination during starvation, CFU/mL was determined by plating serial dilutions.

Acknowledgment. J.S.T. is thankful to Department of Biotechnology (DBT), Government of India, for research funding. G.R.D. thanks the Department of Science and Technology (DST) for the award of a J. C. Bose fellowship. R.K.G. is grateful to DBT for a postdoctoral fellowship and to DST for project funding under Fast track scheme. T.S.T. thanks UGC for the award of a senior research fellowship.

Supporting Information Available: List of 100 top scored compounds obtained from MOE and GOLD docking results. Segregation of top 200 top scored docked compounds into chemical classes (1−11) of similar structural scaffolds. Hydrogen bond analysis of protein ligand interactions for the top scored docked conformation for the biologically active compounds (**5**, **7**, **8**, and **10**). Comparison of secondary structure of the homology model with the X-ray crystal structure crystal structure of DevR (PDB ID: 3C3W). Domain-wise rmsd of Cα atoms of the homology model with the X-ray crystal structure of DevR (PDB ID: 3C3W). Comparison of pocket

used for docking of compounds in homology model with pocket present in crystal structure. Effect of **10** on DevR-regulated promoter activity and viability of *M. tuberculosis* in nutrient starvation model of dormancy. Hydrogen bond interaction array predicted between compounds and DevR. Ligand-based pharmacophore generated from the biologically active ligands based upon maximum feature alignment criteria. Interaction of **10** and DevR in protein model and structure. 3D view of inhibitor (**10**) docked into the putative binding site of the DevR protein. Domains-wise distribution of amino acids in DevR protein, sequence alignment, homology model generation using MOE-homology module, identification of the active site, molecular dynamics, pharmacophore generation, docking. This material is available free of charge via the Internet at http://pubs.acs.org.

References

(1) Parrish, N. M.; Dick, J. D.; Bishai, W. R. Mechanisms of latency in *Mycobacterium tuberculosis*. *Trends Microbiol*. **1998**, *6*, 107–112.
(2) Grange, J. M. The mystery of the mycobacterial "persistor". *Tuberculosis Lung Dis*. **1992**, *73*, 249–251.
(3) Mitchison, D. A. Basic mechanisms of chemotherapy. *Chest* **1979**, *76*, 771–781.
(4) Young, D. B. A post-genomic perspective. *Nat. Med*. **2001**, *7*, 11–13.
(5) Macielag, M. J.; Goldschmidt, R. Inhibitors of bacterial two-component signalling systems. *Expert Opin. Investig. Drugs* **2000**, *9*, 2351–2369.
(6) Stephenson, K.; Hoch, J. A. Two-component and phosphorelay signal-transduction systems as therapeutic targets. *Curr. Opin. Pharmacol*. **2002**, *2*, 507–512.
(7) Tyagi, J. S.; Sharma, D. Signal transduction systems of mycobacteria with special reference to *M. tuberculosis*. *Curr. Sci*. **2004**, *86*, 93–102.
(8) Dasgupta, N.; Kapur, V.; Singh, K. K.; Das, T. K.; Sachdeva, S.; Jyothisri, K.; Tyagi, J. S. Characterization of a two-component system, devR−devS, of *Mycobacterium tuberculosis*. *Tuberculosis Lung Dis*. **2000**, *80*, 141–159.
(9) Park, H. D.; Guinn, K. M.; Harrell, M. I.; Liao, R.; Voskuil, M. I.; Tompa, M.; Schoolnik, G. K.; Sherman, D. R. Rv3133c/dosR is a transcription factor that mediates the hypoxic response of *Mycobacterium tuberculosis*. *Mol. Microbiol*. **2003**, *48*, 833–843.
(10) Ohno, H.; Zhu, G.; Mohan, V. P.; Chu, D.; Kohno, S.; Jacobs, W. R., Jr.; Chan, J. The effects of reactive nitrogen intermediates on gene expression in *Mycobacterium tuberculosis*. *Cell. Microbiol*. **2003**, *5*, 637–648.
(11) Voskuil, M. I.; Schnappinger, D.; Visconti, K. C.; Harrell, M. I.; Dolganov, G. M.; Sherman, D. R.; Schoolnik, G. K. Inhibition of respiration by nitric oxide induces a *Mycobacterium tuberculosis* dormancy program. *J. Exp. Med*. **2003**, *198*, 705–713.
(12) Kumar, A.; Deshane, J. S.; Crossman, D. K.; Bolisetty, S.; Yan, B. S.; Kramnik, I.; Agarwal, A.; Steyn, A. J. Heme oxygenase-1-derived carbon monoxide induces the *Mycobacterium tuberculosis* dormancy regulon. *J. Biol. Chem*. **2008**, *283*, 18032–18039.
(13) Shiloh, M. U.; Manzanillo, P.; Cox, J. S. *Mycobacterium tuberculosis* senses host-derived carbon monoxide during macrophage infection. *Cell Host Microbe* **2008**, *3*, 323–330.
(14) Wayne, L. G.; Sohaskey, C. D. Nonreplicating persistence of Mycobacterium tuberculosis. *Annu. Rev. Microbiol*. **2001**, *55*, 139–163.
(15) Gomez, J. E.; McKinney, J. D. M. Tuberculosis persistence, latency, and drug tolerance. *Tuberculosis (Edinburgh)* **2004**, *84*, 29–44.
(16) Murphy, D. J.; Brown, J. R. Identification of gene targets against dormant phase *Mycobacterium tuberculosis* infections. *BMC Infect. Dis*. **2007**, *7*, 84.
(17) Boon, C.; Dick, T. *Mycobacterium bovis* BCG response regulator essential for hypoxic dormancy. *J. Bacteriol*. **2002**, *184*, 6760–6767.
(18) Saini, D. K.; Tyagi, J. S. High-throughput microplate phosphorylation assays based on DevR−DevS/Rv2027c 2-component signal transduction pathway to screen for novel anti-tubercular compounds. *J. Biomol. Screening* **2005**, *10*, 215–224.
(19) Wisedchaisri, G.; Wu, M.; Rice, A. E.; Roberts, D. M.; Sherman, D. R.; Hol, W. G. Structures of *Mycobacterium tuberculosis* DosR and DosR−DNA complex involved in gene activation during adaptation to hypoxic latency. *J. Mol. Biol*. **2005**, *354*, 630–641.
(20) Wisedchaisri, G.; Wu, M.; Sherman, D. R.; Hol, W. G. Crystal structures of the response regulator DosR from *Mycobacterium tuberculosis* suggest a helix rearrangement mechanism for phosphorylation activation. *J. Mol. Biol*. **2008**, *378*, 227–242.
(21) Gao, R.; Mack, T. R.; Stock, A. M. Bacterial response regulators: versatile regulatory strategies from common domains. *Trends Biochem. Sci*. **2007**, *32*, 225–234.
(22) Irwin, J. J.; Shoichet, B. K. ZINC—a free database of commercially available compounds for virtual screening. *J. Chem. Inf. Model*. **2005**, *45*, 177–182.
(23) Baikalov, I.; Schroder, I.; Kaczor-Grzeskowiak, M.; Cascio, D.; Gunsalus, R. P.; Dickerson, R. E. dimerization? Suggestive evidence from a new crystal form. *Biochemistry* **1998**, *37*, 3665–3676.
(24) Chauhan, S.; Tyagi, J. S. Cooperative binding of phosphorylated DevR to upstream sites is necessary and sufficient for activation of the Rv3134c-devRS operon in *Mycobacterium tuberculosis*: implication in the induction of DevR target genes. *J. Bacteriol*. **2008**, *190*, 4301–4312.
(25) Betts, J. C.; Lukey, P. T.; Robb, L. C.; McAdam, R. A.; Duncan, K. Evaluation of a nutrient starvation model of *Mycobacterium tuberculosis* persistence by gene and protein expression profiling. *Mol. Microbiol*. **2002**, *43*, 717–731.
(26) Sharma, D.; Bose, A.; Shakila, H.; Das, T. K.; Tyagi, J. S.; Ramanathan, V. D. Expression of mycobacterial cell division protein, FtsZ, and dormancy proteins, DevR and Acr, within lung granulomas throughout guinea pig infection. *FEMS Immunol. Med. Microbiol*. **2006**, *48*, 329–336.
(27) Schnappinger, D.; Ehrt, S.; Voskuil, M. I.; Liu, Y.; Mangan, J. A.; Monahan, I. M.; Dolganov, G.; Efron, B.; Butcher, P. D.; Nathan, C.; Schoolnik, G. K. Transcriptional Adaptation of *Mycobacterium tuberculosis* within Macrophages: Insights into the Phagosomal Environment. *J. Exp. Med*. **2003**, *198*, 693–704.
(28) Karakousis, P. C.; Yoshimatsu, T.; Lamichhane, G.; Woolwine, S. C.; Nuermberger, E. L.; Grosset, J.; Bishai, W. R. Dormancy phenotype displayed by extracellular *Mycobacterium tuberculosis* within artificial granulomas in mice. *J. Exp. Med*. **2004**, *200*, 647–657.
(29) Rustad, T. R.; Harrell, M. I.; Liao, R.; Sherman, D. R. The enduring hypoxic response of *Mycobacterium tuberculosis*. *PLoS One* **2008**, *3*, e1502.
(30) Mitchison, D. A. The action of antituberculosis drugs in short-course chemotherapy. *Tubercle* **1985**, *66*, 219–225.
(31) Zhang, Y.; Wade, M. M.; Scorpio, A.; Zhang, H.; Sun, Z. Mode of action of pyrazinamide: disruption of *Mycobacterium tuberculosis* membrane transport and energetics by pyrazinoic acid. *J. Antimicrob. Chemother*. **2003**, *52*, 790–795.
(32) Koul, A.; Vranckx, L.; Dendouga, N.; Balemans, W.; Van den Wyngaert, I.; Vergauwen, K.; Gohlmann, H. W.; Willebrords, R.; Poncelet, A.; Guillemont, J.; Bald, D.; Andries, K. Diarylquinolines are bactericidal for dormant mycobacteria as a result of disturbed ATP homeostasis. *J. Biol. Chem*. **2008**, *283*, 25273–25280.
(33) Andries, K.; Verhasselt, P.; Guillemont, J.; Gohlmann, H. W.; Neefs, J. M.; Winkler, H.; Van Gestel, J.; Timmerman, P.; Zhu, M.; Lee, E.; Williams, P.; de Chaffoy, D.; Huitric, E.; Hoffner, S.; Cambau, E.; Truffot-Pernot, C.; Lounis, N.; Jarlier, V. A diarylquinoline drug active on the ATP synthase of *Mycobacterium tuberculosis*. *Science* **2005**, *307*, 223–227.
(34) Stock, A. M.; Mottonen, J. M.; Stock, J. B.; Schutt, C. E. Three-dimensional structure of CheY, the response regulator of bacterial chemotaxis. *Nature* **1989**, *337*, 745–749.
(35) Boehr, D. D.; Wright, P. E. Biochemistry. How do proteins interact? *Science* **2008**, *320*, 1429–1430.
(36) Marti-Renom, M. A.; Stuart, A. C.; Fiser, A.; Sanchez, R.; Melo, F.; Sali, A. Comparative protein structure modeling of genes and genomes. *Annu. Rev. Biophys. Biomol. Struct*. **2000**, *29*, 291–325.
(37) Thompson, J. D.; Higgins, D. G.; Gibson, T. J. CLUSTAL W: improving the sensitivity of progressive multiple sequence alignment through sequence weighting, position-specific gap penalties and weight matrix choice. *Nucleic Acids Res*. **1994**, *22*, 4673–4680.
(38) Liang, J.; Edelsbrunner, H.; Woodward, C. Anatomy of protein pockets and cavities: measurement of binding site geometry and implications for ligand design. *Protein Sci*. **1998**, *7*, 1884–1897.
(39) Tiwari, A.; Panigrahi, S. K. HBAT: a complete package for analysing strong and weak hydrogen bonds in macromolecular crystal structures. *In Silico Biol*. **2007**, *7*, 651–661.
(40) Bagchi, G.; Chauhan, S.; Sharma, D.; Tyagi, J. S. Transcription and autoregulation of the Rv3134c-devR-devS operon of *Mycobacterium tuberculosis*. *Microbiology* **2005**, *151*, 4045–4053.
(41) Taneja, N. K.; Tyagi, J. S. Resazurin reduction assays for screening of antitubercular compounds against dormant and actively growing *Mycobacterium tuberculosis*, *Mycobacterium bovis* BCG and *Mycobacterium smegmatis*. *J. Antimicrob. Chemother*. **2007**, *60*, 288–293.